Halogen bonding stabilizes a *cis*-azobenzene derivative in the solid state: A crystallographic study

Marco Saccone,[a] Antti Siiskonen,[a] Francisco Fernandez-Palacio,[b] Arri Priimagi,*[a] Giancarlo Terraneo,*[b] Giuseppe Resnati,[b] Pierangelo Metrangolo[b,c]

[a] Department of Chemistry and Bioengineering, Tampere University of Technology, P.O. Box 541, FI-33101 Tampere, Finland

[b] Laboratory of Nanostructured Fluorinated Materials (NFMLab), Department of Chemistry, Materials, and Chemical Engineering "Giulio Natta", Politecnico di Milano, Via L. Mancinelli 7, 20131 Milano, Italy

[c] HYBER Centre of Excellence, Department of Applied Physics, Aalto University, P.O. Box 15100, FI-02150, Espoo, Finland

Correspondence to: arri.priimagi@tut.fi and giancarlo.terraneo@polimi.it

Crystals of *trans*- and *cis*-isomers of a fluorinated azobenzene derivative have been prepared and characterized by single crystal X-ray diffraction. The role of the halogen bond in stabilizing the *cis* form is inferred by the packing analysis and by theoretical calculations. Due to the rarity of *cis*-azobenzene crystal structures in the literature, our paper makes a step towards understanding the role of non-covalent interactions in driving the packing of metastable azobenzene isomers. This is expected to be important in the future rational design of solid-state, photoresponsive materials based on halogen bonding.

Introduction

Azobenzenes are molecules containing two aromatic rings held together by a nitrogen-nitrogen double bond. Due to the N=N link, they exist in two stereoisomeric forms, *trans* and *cis*, and it is possible to switch the former to the latter and *vice versa* by absorption of UV-visible photons (Zhao & Ikeda, 2009; Dhammika Bandara & Burdette, 2012). The *trans*-form is usually more thermodynamically stable than the *cis*-form, which is usually kinetically not persistent in ambient conditions (Hoffmann, 1987; Hoffmann *et al*., 2008). Recently there has been considerable interest towards long-lived *cis*-azobenzenes from the perspective of making bi-stable systems that can be reversibly switched with light (Bléger & Hecht, 2015; Beharry *et al.*, 2011; Weston *et al.*, 2014). For example, Woolley and collaborators, based on previous work of Herges *et al.,* (Siewertsen *et al.*, 2009), reported on the exceptional photoswitching behavior of the 5,6-dihydrodibenzo[*c*,*g*][1,2]diazocine (**Fig. 1**a) that has been used to exert a reversible and efficient photocontrol over the conformation of a peptide (Samanta *et al*., 2012). In their case the *cis*-form is the more thermodynamically stable isomer. More recently Bléger and coworkers showed that the *cis*-forms of some *ortho*-fluorinated azobenzenes (**Fig. 1**b) possess an impressive kinetic stability in solution, with *cis*-*trans* thermal lifetimes up to several months or even a year (Bléger *et al*., 2012; Knie *et al.*, 2014).

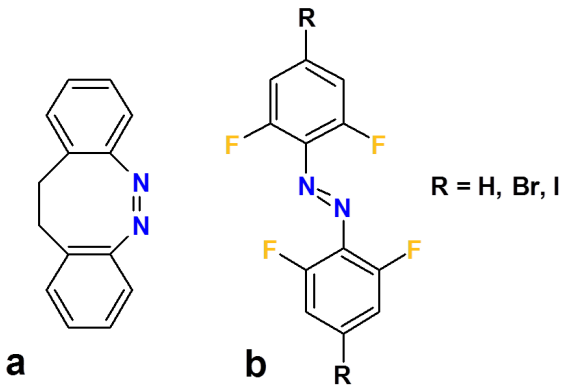

Fig. 1: Examples of molecules having a kinetically persistent *cis* isomer.

Barrett *et al.* have used the aforementioned *ortho*-fluorinated azobenzenes to produce mechanical motion upon irradiation of an azobenzene crystal. The mechanical motion has been attributed to the isomerization of the azobenzenes in the crystalline state (Bushuyev, Corkery *et al*., 2014; Bushuyev, Tomberg *et al*., 2014). Our interest in fluorinated azobenzenes started in 2012 when we developed halogen-bonded photoresponsive polymeric and liquid-crystalline materials, demonstrating that halogen bonding is an efficient supramolecular tool for light-induced surface patterning and photoalignment (Priimagi, Cavallo *et al.*, 2012; Priimagi, Saccone *et al.*, 2012; Saccone, Cavallo *et al*., 2015). Subsequently, we developed a small library of halogen-bonded liquid crystals based on fluorinated azobenzenes that undergo a rich variety of photoinduced phase transitions upon light irradiation (Fernandez-Palacio, Poutanen *et al*., 2016). These results were achieved thanks to the unique characteristics of halogen bonding, namely its strength and directionality (Saccone *et al*., 2013) that allows this interaction to influence the solid-state structure even in the presence of competing stronger interactions (Corradi *et al*., 2000). Given the fact that many intriguing applications, *e.g.,* fabrication of bistable light-activated devices, depend on properties of the azobenzene molecules in the solid state, it is perhaps surprising that the solid-state structural analysis of *cis*-azobenzenes is rather unexplored. The fact that only 30 crystal structures of azobenzene in the *cis* form are present in the Cambridge Structural Database (Bushuyev *et al*., 2015), of which about half are fluorinated, is a good indication of the importance of fluorination in the design of azobenzene molecules having a kinetically persistent *cis*-form.

Herein, we report the structural analysis of both *trans*- and *cis*-isomers, labeled here **TRANS**$_{azo}$ and **CIS**$_{azo}$, of the fluorinated azobenzene shown in **Fig. 2**. We show that halogen bonding plays an important role in the stabilization of the *cis*-isomer in the solid state while in the *trans*-isomer, no halogen bond is detected. Our analysis is complemented by theoretical calculations that shed further light on the experimental data.

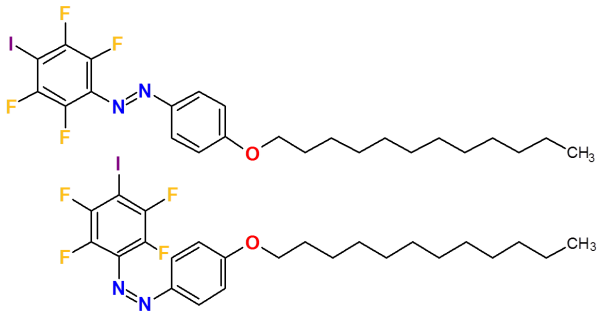

Fig. 2: The **TRANS**$_{azo}$(top) and **CIS**$_{azo}$ (bottom) isomers of the azobenzene studied in the present work.

Experimental

Materials

The **TRANS**$_{azo}$ molecule was synthesized as previously reported (Fernandez-Palacio, Poutanen *et al*., 2016). Its photoisomerization properties have been studied in dilute dimethylformamide solution upon irradiation with UV light (365 nm), and the lifetime of the *cis*-isomer was found to be *ca*. 12 days (Fernandez-Palacio, Poutanen *et al*., 2016). The long *cis*-lifetime enabled us to obtain crystals of **CIS**$_{azo}$, upon illumination at 395 nm wavelength of a concentrated solution of **TRANS**$_{azo}$ and subsequent solvent evaporation. Single crystals suitable for X-ray diffraction studies were obtained for both isomers by slow evaporation from chloroform solutions. The evaporation took place in dark in order to prevent unwanted isomerization caused by ambient light, especially pertinent for obtaining the **CIS**$_{azo}$ crystals.

Computational details

Geometry minimization and complexation energy calculations were performed with Gaussian 09 Revision D.01 (Frisch *et al*., 2009). The Quantum Theory of Atoms in Molecule (QTAIM) and Interacting Quantum Atoms (IQA) analyses was performed with AIMAll version 16.10.31 (Keith, 2016). The geometries were optimized on a potential energy surface corrected for the basis set superposition error (BSSE) using the counterpoise method implemented in Gaussian 09 (Boys & Bernardi, 1970). A frequency calculation was performed after the geometry minimization in order to confirm that the obtained geometry is a true minimum (i.e. no imaginary frequencies). M06-2X/DGDZVP method was used for geometry optimization and to calculate the complexation energy (Siiskonen & Priimagi, 2017). To speed up the calculation, the long alkyl chain was truncated to methyl. M06-2X/def2-TZVP method and the atom coordinates from the crystal structure were used to obtain the wavefunction for the QTAIM analysis.

Structure determination

The crystal data, data collection and structure refinement details are summarized in **Table 1**. The crystals were mounted in inert oil on glass fibers. Data were collected on a Bruker Kappa APEXII CCD diffractometer with Mo *Kα* radiation (λ = 0.7107 Å) and a Bruker Kryoflex low-temperature device.

Table 1

Experimental details

	TRANS$_{azo}$	**CIS**$_{azo}$
Crystal data		
Chemical formula	$C_{24}H_{29}F_4IN_2O$	$C_{24}H_{29}F_4IN_2O$
M_r	564.39	564.39
Crystal system, space group	*Triclinic,* *P-1*	*Monoclinic,* *$P2_1/c$*
Temperature	103(2)	103(2)
a, b, c (Å)	7.4374(9), 10.2935(12), 16.536(2)	8.5802(16), 33.663(5), 8.752(2)
α, β, γ (°)	105.237(10), 101.641(10), 95.607(12)	90.00, 109.255(16), 90.00
V (Å^3)	1181.0(2)	2386.5(8)
Z	2	4
Radiation type	Mo $K\alpha$	Mo $K\alpha$
μ (mm^{-1})	1.406	1.391
Crystal size (mm)	0.40 x 0.25 x 0.05	0.20 x 0.10 x 0.05
Data collection		
Diffractometer	Bruker Kappa Apex II	Bruker Kappa Apex II
Absorption correction	Multi-scan SADABS (Brucker, 2008)	Multi-scan SADABS (Brucker, 2008)
T_{min}, T_{max}	0.553, 0.706	0.791, 0.862
No. of measured, independent and observed [$I > 2\sigma(I)$] reflections	39236, 10045, 8800	25224, 5073, 3840
R_{int}	0.028	0.047
(sin $\theta/\lambda)_{max}$ (Å^{-1})	0.822	0.650
Refinement		
R [$F^2 > 2\sigma(F^2)$], $wR(F^2)$, S	0.030, 0080, 1.07	0.037, 0.059, 1.05
No. of reflections	10045	5073
No. of parameters	290	290
No. of restraints	0	0
H-atom treatment	H-atom parameters not refined	H-atom parameters not refined
$\Delta\rho_{max}$, $\Delta\rho_{min}$ (e Å^{-3})	1.39, -1.72	0.57, -0.99

Computer programs: APEX2, SAINT, SADABS (Bruker, 2008), SIR2002 (Burla et al., 2003), SHELXL97 (Sheldrick, 2008), Mercury (Macrae et al., 2008).

Results and discussion

Structural analysis of ***TRANS***$_{azo}$

The molecule **TRANS**$_{azo}$ has been originally conceived with the purpose of obtaining a promesogenic molecule which, thanks to the halogen bond (Cavallo *et al.*, 2016), would produce supramolecular halogen-bonded liquid crystals featuring photoinduced phase transitions (Fernandez-Palacio, Poutanen *et al.*, 2016). Its structural design combines halogen-bond-donating capability, long lifetime of the *cis*-isomer, and a long aliphatic chain which typically promotes the appearance of liquid-crystal phases. The molecule crystallizes in the *P-1* space group with the azo group exclusively adopting the *trans* configuration (**Fig. 3b**). The two benzene rings are not coplanar and the angle between them is 9.7°.

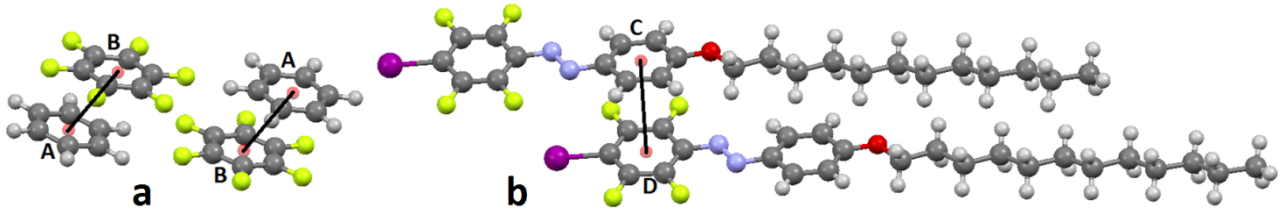

Fig. 3: Arene-perfluoroarene quadrupolar interactions as observed in **BICVUE01** (**a**) and **TRANS**$_{azo}$, (**b**). The red dots denote the centroids of the aromatic rings.

The crystal packing is mainly driven by two kinds of intermolecular interactions. One of them is the arene-perfluoroarene quadrupolar interaction that occurs between molecules in neighboring planes. The observed distance between the centroids of the fluorinated and non-fluorinated rings is 3.72 Å, very close to that of the benzene-hexafluorobenzene dimer (**Fig. 3a**) (Williams *et al*., 1992). This interaction may be strong, 6.1 kcal mol^{-1} for the benzene-hexafluorobenzene adduct (Řezáč *et al*., 2012), and is very useful in crystal engineering (Salonen *et al*., 2011), as well as in liquid-crystal self-assembly (Kishikawa, 2012). It is interesting to observe that the similarities in the crystals packing of the **TRANS**$_{azo}$ and the benzene-hexafluorobenzene dimer **BICVUE01** extend also to the arrangement of the aromatic rings in neighboring planes as depicted in **Fig. 4**.

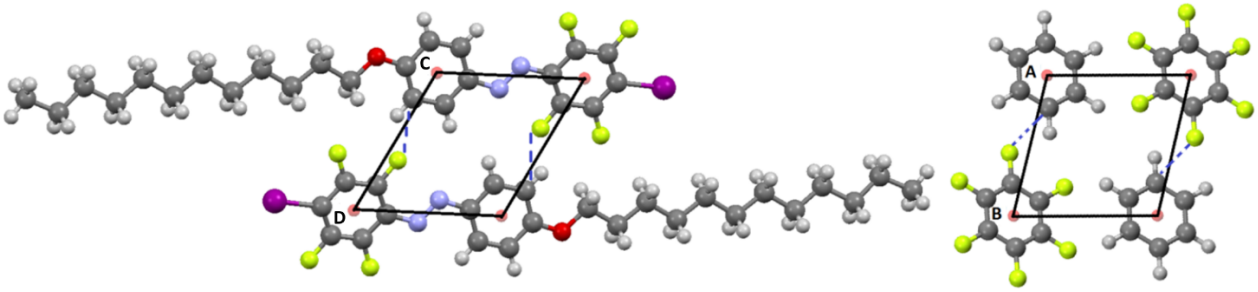

Fig. 4: The arrangement of the aromatic rings is similar in **TRANS**$_{azo}$ (left) and in **BICVUE01** (right). The red dots denote the centroids of the aromatic rings. **CD** distance is 6.82 Å and **AB** distance is 6.85 Å. The view is along the *c* axis. H···F hydrogen bonds are denoted with dotted blue lines.

Secondly, the molecular arrangement is promoted by H9···F1$_{(-x, -y, -z)}$ hydrogen bond having the following geometrical parameters: C···F distance of 3.1477(17) Å; C-H···F angle of 118°, which appear to be very similar in both structures (**Fig. 4**). In addition, the iodofluorinated ring further interacts with other neighboring molecules. Specifically, two fluorine atoms show weak hydrogen bond contacts with hydrogen atoms located at the terminal part of the aliphatic chains and the iodine atom points toward the methyl unit on the translated molecules (-4+x, y, -1+z). Finally, the crystal packing is stabilized by several C-H$_{(aliph)}$···C-H$_{(aliph)}$ interactions that induce the segregation of neighboring aliphatic chains from the azobenzene cores (**Fig. 5**). We have recently observed a similar segregation of aliphatic moieties from aromatic cores in a co-crystal structure where the **TRANS**$_{azo}$ molecule is combined with a 4,4'-alkoxystilbazole derivative (Fernandez-Palacio, Poutanen *et al.*, 2016), shown to be important when developing materials possessing liquid-crystalline properties (Tschierske, 2012). In the present structure, the iodine atom is not involved in any particular intermolecular interaction, and even the electron-rich nitrogen atoms of the azo-group are non-interacting, as derived by metric analysis. In contrast, the **CIS**$_{azo}$ structure is profoundly influenced by iodine-nitrogen interactions, as described below.

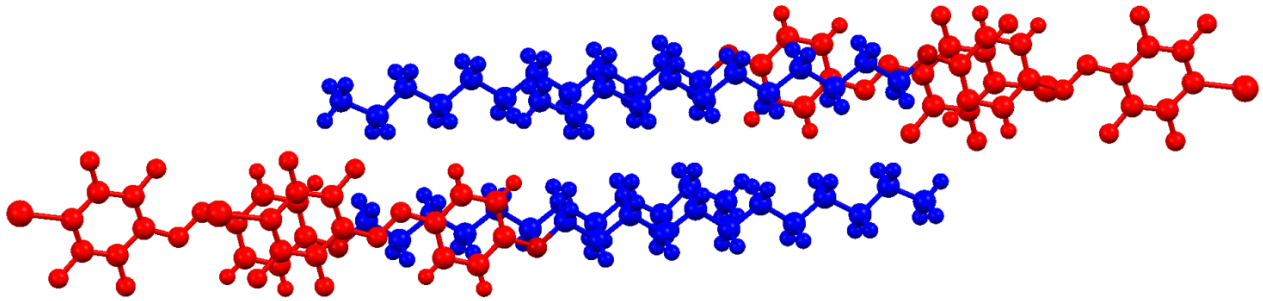

Fig. 5: A view along the c axis of the overall packing of **TRANS**$_{azo}$ molecules, showing the segregation of the aliphatic regions (depicted in blue) from the aromatic cores (depicted in red).

*Structural analysis of **CIS**$_{azo}$*

The **CIS**$_{azo}$ molecule is a metastable isomer of the **TRANS**$_{azo}$ molecule and its lifetime (*ca*. 12 days in DMF solution), increased by fluorination, was long enough to allow us to prepare the *cis* single crystals and study their structural properties by X-ray diffraction analysis. Recently, the structure of some fluorinated *cis*-azobenzenes have been reported (Bushuyev, Corkery *et al*., 2014; Bushuyev, Tomberg *et al*., 2014), however, these papers concentrate solely on symmetrically substituted azobenzenes that lack long alkyl chains. This usually simplifies the crystallization process, but does not allow to infer the role of interactions that do not involve the aromatic moieties in the crystal packing. We address this issue in our analysis. The **Cis**$_{azo}$ form crystallizes in the *P2$_1$/c* space group with the azo group quantitatively adopting the *cis*-form. The overall packing of the **CIS**$_{azo}$ molecule features several differences compared to the **TRANS**$_{azo}$. The most significant difference seems to be the presence of halogen bonding between the iodine atom in the tetrafluorophenyl

ring and one of the nitrogen atoms of the azo moiety of another molecule in the same plane (**Fig. 6a**). The N···I distance is 2.995 Å, corresponding to 16% reduction in the sum of the van der Waals radii of I and N (Bondi, 1964) and the C-I···N angle is approximately 170.2°. The adopted *cis*-form makes the nitrogen lone pair more accessible to interact with the Lewis-acidic iodine atom, transforming the azo unit into a fairly good halogen-bond acceptor (**Fig. 6a**). This contact is quite short and comparable to the similar ones reported in the literature, for instance in the complex between in diazobicyclooctane and CBr_4 (Blackstock *et al.*, 1987) or in a metal-organic coordination polymer (Fernandez-Palacio, Saccone *et al.*, 2016). The strength of the observed halogen bonding has been estimated by theoretical calculations at the density functional level to be around 4.38 kcal/mol. The effectiveness of the iodine atom as a halogen-bond donor is further highlighted by the molecular electrostatic potential of **CIS**$_{azo}$ (**Fig. 6**b) where the positive σ-hole on the iodine atom located on the extension of the C-I bond (Politzer *et al.*, 2007), and the negative area associated to the lone pairs of the azo group, are clearly evident.

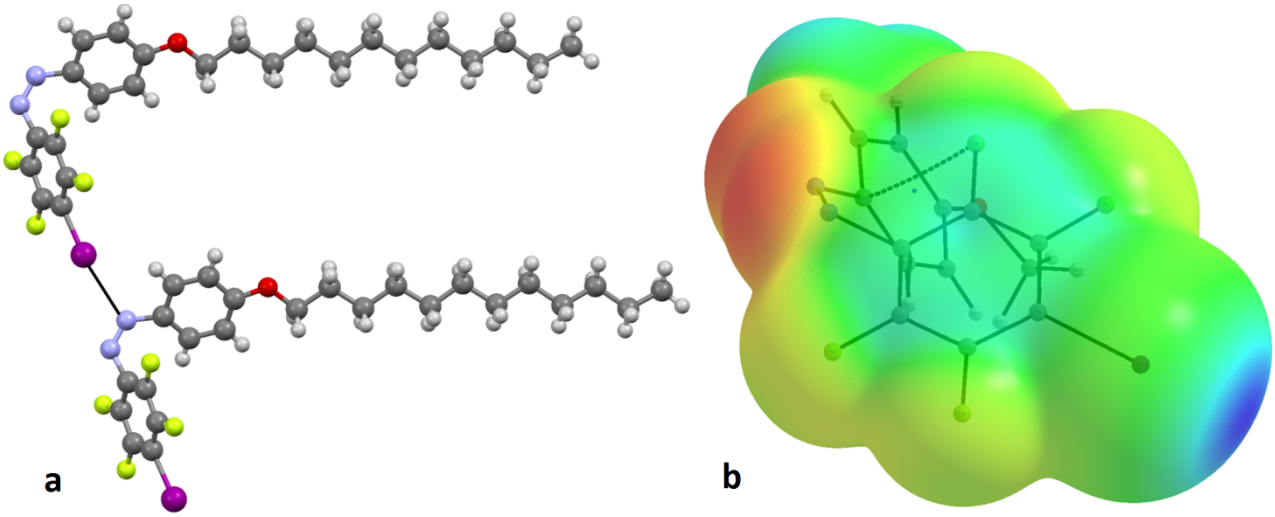

Fig. 6: The N···I halogen bond between the iodine atom and a nitrogen in the azo group (**a**), and the electrostatic potential of **CIS**$_{azo}$ computed at the 0.001 au of the electron density contour. Negative potential areas colored in red-yellow, positive potential areas colored in blue-cyan (**b**).

Similar to the **TRANS**$_{azo}$ derivative, in the packing of **CIS**$_{azo}$ a strong tendency of the aliphatic chains towards phase segregation is observed (**Fig. 7a**). Conversely, no arene-perfluoroarene quadrupolar interactions are detected (**Fig. 7b**). These observations further strengthen the finding that halogen bonding is one of the main driving forces of the molecular packing of the **CIS**$_{azo}$ molecule.

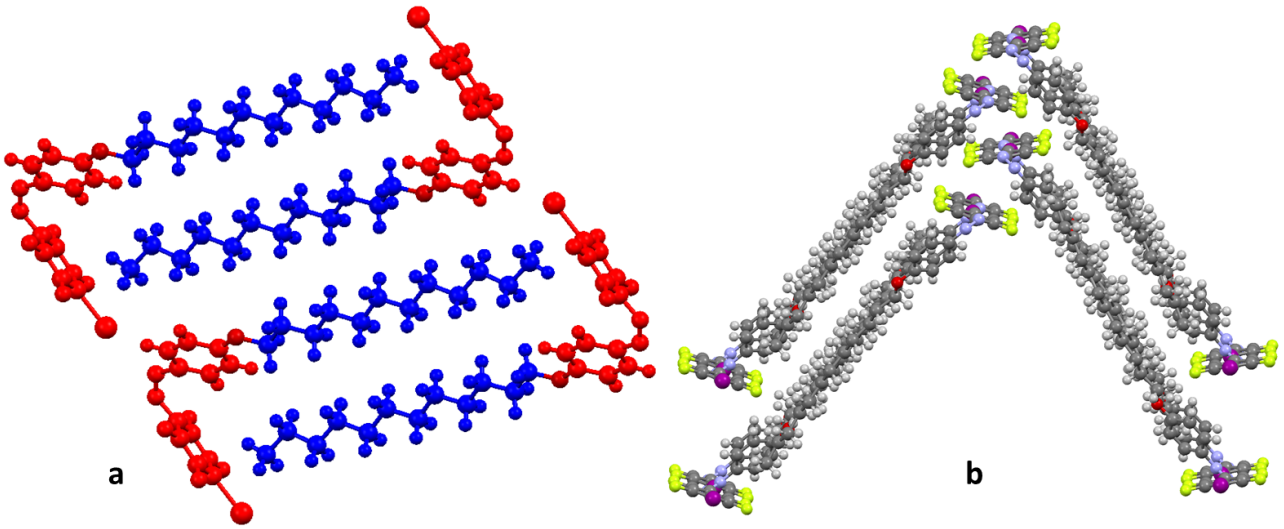

Fig. 7: **a**, Two-dimensional (along the b axis)**,** and **b**, three-dimensional view of the crystals packing of **CIS**$_{azo}$. The segregation of the aliphatic chains (blue) from the aromatic regions (red) is evident from **a**, furthermore the perfluorinated rings do not closely interact with the non-fluorinated rings as depicted in **b**.

Defining the two planes containing either aromatic rings, a tilt angle of 61.6° is observed between them. Due to the tilting of the rings, one of the *ortho*-substituents in both rings is located quite close to the *ipso*-carbon of the adjacent ring. The distance between one of the *ortho*-fluorines and the *ipso*-carbon is 2.839 Å, which is less than the sum of their van der Waals radii (3.17 Å). The same holds for the distance between one of the *ortho*-hydrogens and the *ipso*-carbon (2.501 Å; the sum of the vdW radii is 2.90 Å). In fact, the quantum theory in atom in molecules (QTAIM) (Bader, 1991) analysis shows two unusual bond critical points, indicating a bonding interaction between the *ortho*-substituents and the *ipso*-carbons (**Fig. 8**). Interacting quantum atoms (IQA) (Blanco *et al*., 2004; Francisco *et al*., 2006) analysis was performed to further study these bonding interactions.

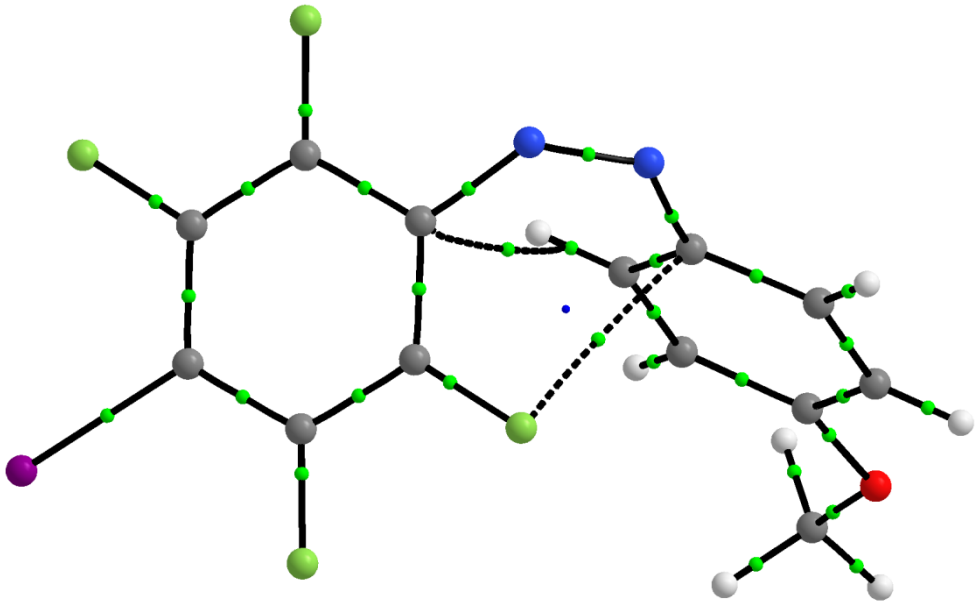

Fig. 8: QTAIM analysis of the **CIS**$_{azo}$ molecule. Bond critical points are shown as green dots.

The most relevant values of the QTAIM and IQA analyses are presented in **Table 2**. The small, positive values for the electron densities (ρ) and the Laplacians of the electron densities ($\nabla^2\rho$) at the aforementioned bond critical points indicate that the interactions are of weak, closed-shell type. The negative interaction energies (E_{inter}) suggest that the interactions are stabilizing, and that the C···F interaction is significantly stronger than the C···H interaction. The interaction energies have been further divided into electrostatic (E_{cl}) and exchange (E_x) components. The comparison of the components show that the stabilizing energy of the C···F interaction is mainly due to the classical electrostatic, or Coulombic, energy component with only a small contribution from the exchange energy component. The energy of the much weaker C···H interaction, however, is mainly due to the exchange energy component. Even if further studies are needed to support this claim, we believe that such stabilizing C···F interaction plays an important role in dictating the unprecedented stability of the *cis*-forms of fluorinated azobenzenes (Bléger *et al*., 2012; Knie *et al.*, 2014).

Table 2

IQA and QTAIM analysis

Interaction	ρ(BCP)	$\nabla^2\rho$(BCP)	E_{inter}	E_{cl}	E_x
C···F	0.0108	0.0470	-24.10	-19.89	-4.21
C···H	0.0133	0.0472	-5.08	-1.76	-3.32

Conclusions

We have reported the crystal structures of *trans*- and *cis*-isomers of a fluorinated azobenzene shown in **Fig. 1**. The analysis of their structures in the solid state revealed an arrangement of the molecules that is profoundly different for the two isomers. In the *cis*-isomer structure, halogen bonding between neighboring molecules provides a stabilizing contribution to the overall packing, while in the *trans*-isomer, a major contribution is given by arene-perfluoroarene quadrupolar interactions. Due to the rarity of *cis*-azobenzene structures in the literature, our investigation is a step forward towards more comprehensive understanding of the role of non-covalent interactions in driving the crystal packing of metastable isomers of photoresponsive molecules.

Acknowledgments

A. P. gratefully acknowledges the Academy of Finland Research Fellowship program (Decision Nos. 277091 and 284553), and the Emil Aaltonen Foundation for financial support. A. S. is thankful to Prof. Ángel Martín Pendás for helpful discussions regarding the Interacting Quantum Atoms analysis.

References

(1) Bader, R. F. W. (1991). *Chem. Rev*. **91**, 893-928.

(2) Beharry, A. A., Sadovski, O. & Woolley, A. G. (2011). *J. Am. Chem. Soc.*, **133**, 19684-19687.

(3) Blackstock, S.C. & Kochi, J. K. (1987). *J. Am. Chem. Soc.*, **109**, 2484-2496.

(4) Blanco, M. A., Martín Pendás, A. & Francisco, E. (2004). *J. Chem. Theory Comput.*, **1**, 1096-1109.

(5) Bléger, D., Schwarz, J., Brouwer, A. M. S. & Hecht, S. (2012). *J. Am. Chem. Soc*., **134**, 20597-20600.

(6) Bléger, D. & Hecht, S. (2015). *Angew. Chem. Int. Ed*., **54**, 11338-11348.

(7) Bondi, A. (1964). *J. Phys. Chem*., **68**, 441-451.

(8) Boys S. F. & Bernardi F. (1970). *Mol. Phys.*, **19**, 553–566.

(9) Bruker (2008). *APEX2*, *SAINT* and *SADABS*. Bruker AXS Inc. Madison, Wisconsin, USA.

(10) Burla, M. C., Camalli, M., Carrozzini, B., Cascarano, G. L., Giacovazzo, C., Polidori, G. & Spagna, R. (2003). *J. Appl. Cryst*. **36**, 1103.

(11) Bushuyev, O. S., Tomberg, A., Friščić, T. & Barrett, C. J. (2014). *J. Am. Chem. Soc*., **135**, 12556-12559.

(12) Bushuyev, O. S., Corkery, T. C., Barrett, C. J. & Friščić, T. (2014). *Chem. Sci*., **5**, 3158-3164.

(13) Bushuyev, O. S., Tan, D., Barrett, C. J. & Friščić, T. (2015). *CrystEngComm*, **17**, 73-80.

(14) Cavallo, G., Metrangolo, P., Milani, R., Pilati, T., Priimagi, A., Resnati, G. & Terraneo G. (2016). *Chem. Rev*., **116**, 2478-2601.

(15) Corradi, E., Meille, S. V., Messina, M. T., Metrangolo, P. & Resnati, G. (2000). *Angew. Chem. Int. Ed.*, **39**, 1782-1786.

(16) Dhammika Bandara, H. M. & Burdette, S. C. (2012). *Chem. Soc. Rev.*, **41**, 1809-1825.

(17) Fernandez-Palacio, F., Saccone, M., Priimagi, A., Terraneo, G., Pilati, T., Metrangolo, P. & Resnati, G. (2016). *CrystEngComm*, **18**, 2251-2257.

(18) Fernandez-Palacio, F., Poutanen, M., Saccone, M., Siiskonen, A., Terraneo, G., Resnati, G., Ikkala, O., Metrangolo, P. & Priimagi A. (2016). *Chem. Mater.*, **28**, 8314-8321.

(19) Francisco, E., Martín Pendás, A. & Blanco, M. A. (2006). *J. Chem. Theory Comput.*, **2**, 90-102.

(20) Frisch, M. J., Trucks, G. W., Schlegel, H. B., Scuseria, G. E., Robb, M. A., Cheeseman, J. R., Scalmani, G., Barone, V., Mennucci, B., Petersson, G. A., Nakatsuji, H., Caricato, M., Li, X., Hratchian, H. P., Izmaylov, A. F., Bloino, J., Zheng, G., Sonnenberg, J. L., Hada, M., Ehara, M., Toyota, K., Fukuda, R., Hasegawa, J., Ishida, M., Nakajima, T., Honda, Y., Kitao, O., Nakai, H., Vreven, T., Montgomery, J. A., Jr., Peralta, J. E., Ogliaro, F., Bearpark, M., Heyd, J. J., Brothers, E., Kudin, K. N., Staroverov, V. N., Kobayashi, R., Normand, J., Raghavachari, K., Rendell, A., Burant, J. C., Iyengar, S. S., Tomasi, J., Cossi, M., Rega, N., Millam, J. M., Klene, M., Knox, J. E., Cross, J. B., Bakken, V., Adamo, C., Jaramillo, J., Gomperts, R., Stratmann, R. E., Yazyev, O., Austin, A. J., Cammi, R., Pomelli, C., Ochterski, J. W., Martin, R. L., Morokuma, K., Zakrzewski, V. G., Voth, G. A., Salvador, P., Dannenberg, J. J., Dapprich, S., Daniels, A. D., Farkas, Ö., Foresman, J. B., Ortiz, J. V., Cioslowski, J. & Fox, D. J. (2009). Gaussian 09, Revision D.01, Gaussian, Inc., Wallingford CT.

(21) Hoffmann, R. (1987). *Am. Sci*., **75**, 619-621.

(22) Hoffmann, R., Schleyer, P. W. R. & Schaefer III, H. F. (2008). *Angew. Chem. Int. Ed*., **47**, 7164-7167.

(23) Keith, T. A. (2016). TK Gristmill Software, Overland Park KS, USA, (aim.tkgristmill.com)

(24) Kishikawa, K. (2012). *Isr. J. Chem*., **52**, 800-808.

(25) Knie, C., Utecht, M., Zhao, F., Kulla, H., Kovalenko, S., Brouwer, A. M., Saalfrank, P., Hecht, S. & Bléger, D. (2014). *Chem. Eur. J*., **20**, 16492-16501.

(26) Macrae, C. F., Bruno, I. J., Chisholm, J. A., Edgington, P. R., McCabe, P., Pidcock, E., Rodriguez-Monge, L., Taylor, R., van de Streek, J. & Wood, P. A. (2008). *J. Appl. Cryst*. **41**, 466–470.

(27) Politzer, P., Lane, P., Concha, M. C., Ma, Y. & Murray, J. S. (2007). *J. Mol. Model*., **13**, 305-311.

(28) Priimagi, A., Cavallo, G., Forni, A., Gorynsztejn-Leben, M., Kaivola, M., Metrangolo, P., Milani, R., Shishido, A., Pilati, T., Resnati, G. & Terraneo, G. (2012) Adv. Funct. Mater. **22**, 2572-2579.

(29) Priimagi, A., Saccone, M., Cavallo, G., Shishido, A., Pilati, T., Metrangolo P. & Resnati, G. (2012). *Adv. Mater*., **24**, OP345-352.

(30) Řezáč, J., Riley, K. E. & Hobza, P. (2012) *J. Chem. Theory Comput*., **8**, 4285-4292.

(31) Saccone, M., Cavallo, G., Metrangolo, P., Pace, A., Pibiri, A., Pilati, T., Resnati G. & Terraneo G. (2013). *CrystEngComm*, **15**, 3102-3105.

(32) Saccone, M., Cavallo, G., Metrangolo, P., Resnati G. & Priimagi, A. (2015). *Top. Curr. Chem*., **359**, 147-166.

(33) Salonen, L. M., Ellermann, M. & Diederich, F. (2011) *Angew. Chem. Int. Ed*., **50**, 4808-4842.

(34) Samanta, S., Qin, C., Lough, A. J. & Woolley, A. (2012). *Angew. Chem. Int. Ed*., **51**, 6452-6455.

(35) Sheldrick, G. M. (2008). *Acta Cryst. A***64**, 112–122.

(36) Siewertsen, R., Neumann, H., Buchheim-Stehn, B., Herges, R., Näther, C., Renth F. & Temps, F. (2009). *J. Am. Chem. Soc*., **131**, 15594-15595.

(37) Siiskonen, A & Priimagi, A. (2017). J. Mol. Model., submitted.

(38) Tschierske, C. (2012). *Top. Curr. Chem.*, **318**, 1-108.

(39) Weston, C. E., Richardson, R. D., Haycock, P. R., White, A. J. P. & Fuchter, M. J. (2014). *J. Am. Chem. Soc*., **136**, 11878-11881.

(40) Williams, J. H., Cockcroft, J. K. & Fitch, A.N. *Angew. Chem. Int. Ed.*, **1992**, *31*, 1655-1657.

(41) Zhao, Y. & Ikeda, T. (2009). *Smart Light-Responsive Materials: Azobenzene-Containing Polymers and Liquid Crystals*, Wiley, New York.